

## SPECTROSCOPY OF PLUTO AND TRITON AT 3–4 MICRONS: POSSIBLE EVIDENCE FOR WIDE DISTRIBUTION OF NONVOLATILE SOLIDS

W. M. GRUNDY,<sup>1</sup> M. W. BUIE,<sup>1</sup> AND J. R. SPENCER

Lowell Observatory, 1400 West Mars Hill Road, Flagstaff, AZ 86001; grundy@lowell.edu

Received 2002 April 24; accepted 2002 July 8

### ABSTRACT

We present new albedo spectra of Triton and Pluto-Charon, covering the 2.8–4.1  $\mu\text{m}$  wavelength range at a spectral resolution of  $\sim 60$ . The new data reveal three strong  $\text{CH}_4$  ice absorption bands, as well as additional absorption around 2.9 and 4.1  $\mu\text{m}$  in the spectra of both bodies, which we tentatively attribute to widely distributed  $\text{H}_2\text{O}$  ice, along with  $\text{CO}_2$  and/or  $\text{SO}_2$  ices. Since these species are nonvolatile at typical Triton and Pluto surface temperatures, widespread distribution of any of them in volatile-rich regions challenges current understanding of the surfaces of Pluto and Triton, in which more volatile, mobile ices are thought to be segregated from less volatile species. Our data suggest that small, nonvolatile ice particles on Triton and Pluto may be undergoing redistribution by aeolian transport in seasonal sublimation winds.

*Key words:* planets and satellites: individual (Pluto, Triton)

### 1. INTRODUCTION

Most of what is currently known about the surface compositions of Pluto and Triton has been derived from spectroscopic observations at wavelengths ranging from the visible to 2.5  $\mu\text{m}$ , where ices such as  $\text{N}_2$ ,  $\text{CH}_4$ ,  $\text{CO}_2$ ,  $\text{CO}$ , and  $\text{H}_2\text{O}$  exhibit distinctive patterns of vibrational overtone absorption bands (e.g., Cruikshank et al. 1993; Owen et al. 1993; Schmitt et al. 1998; Douté et al. 1999; Quirico et al. 1999; Cruikshank et al. 2000). At continuum near-infrared wavelengths between absorption bands, grains or fractures in surfaces composed of these ices efficiently scatter incident sunlight, facilitating remote observation of the contrast between bands and continuum wavelengths. The observations are modeled by means of multiple-scattering radiative transfer models, typically those of Hapke (1993) and Douté & Schmitt (1998). Based on this approach, the general picture that has emerged over the past two decades is one in which volatile  $\text{N}_2$  ice is in vapor-pressure equilibrium with a nitrogen-rich atmosphere. Solar heating drives  $\text{N}_2$  ice sublimation, followed by recondensation in regions currently receiving less sunlight. This volatile transport probably produces complex, seasonally varying patterns of  $\text{N}_2$  ice distribution. Other volatile ices such as  $\text{CH}_4$  and  $\text{CO}$  are partially soluble in  $\text{N}_2$  ice, but being less volatile, they are preferentially left behind when  $\text{N}_2$  sublimates. On Pluto,  $\text{CH}_4$  is sufficiently abundant to saturate  $\text{N}_2$  ice, and a significant fraction of the observed  $\text{CH}_4$  on Pluto exists as  $\text{CH}_4$  ice I (Owen et al. 1993; Douté et al. 1999), rather than strictly as a minority solute in  $\text{N}_2$  ice, as it does on Triton (Cruikshank et al. 1993; Quirico & Schmitt 1997a; Quirico et al. 1999). The behavior of  $\text{CO}$  ice is less well constrained, since it has fewer near-infrared absorption bands than  $\text{CH}_4$ . However, recent observations show that  $\text{CO}$  on Pluto's surface is distributed differently from  $\text{N}_2$  and  $\text{CH}_4$  ices (Grundy & Buie 2001).

The seasonal cycles of volatile transport are thought to take place on a relatively immobile substrate of nonvolatile ices, the composition of which includes  $\text{H}_2\text{O}$  and  $\text{CO}_2$  on

Triton (Cruikshank et al. 1993; Quirico et al. 1999; Cruikshank et al. 2000). Pluto's substrate composition is less certain, but it probably includes  $\text{H}_2\text{O}$  ice (Grundy & Buie 2002). Additionally, various complex carbonaceous and nitrile species are thought to occur on Triton and Pluto, resulting from photolysis and radiolysis of simpler, more volatile molecules (e.g., Delitsky & Thompson 1987; Bohn et al. 1994).

Relatively few observations have been undertaken at wavelengths longer than 2.5  $\mu\text{m}$  because of difficulties arising from decreasing solar flux, increasing telluric sky brightness, and scarcity of suitable instrumentation. However, longer wavelengths offer several potential advantages. The fundamental vibrational transitions of many ice species are located in this region. Their absorptions are much stronger than the overtone transitions observed shortward of 2.5  $\mu\text{m}$ , opening the possibility of detecting additional minority species, as well as better constraining the distributions of known ices. Many strong, narrow gas-phase absorptions occur in this region as well, offering the possibility of directly measuring atmospheric compositions, if spectra can be obtained with sufficient spectral resolution.

Spencer, Buie, & Bjoraker (1990) obtained photometric observations of Pluto and Triton through four filters spanning the 2.8–4  $\mu\text{m}$  range. They found strong absorption around 3.2  $\mu\text{m}$ , consistent with the  $\nu_3$  absorption band of  $\text{CH}_4$  ice, but the spectral resolution of the data was insufficient to yield additional compositional constraints beyond what had already been ascertained from shorter wavelength observations (e.g., Buie & Fink 1987; Cruikshank et al. 1989).

### 2. OBSERVATIONS

Observations of Triton and Pluto-Charon were obtained during 2000 July 18–22 UT at NASA's IRTF (Infrared Telescope Facility) on Mauna Kea, using the newly commissioned SpeX infrared spectrometer (Rayner et al. 1998). This instrument/telescope combination provides high-throughput, simultaneous recording of medium spectral resolution spectroscopy over a broad wavelength range, at an excellent infrared observing site. With these capabilities, we

<sup>1</sup> Visiting Astronomer at the Infrared Telescope Facility, which is operated by the University of Hawaii under contract with NASA.

TABLE 1  
MIDOBSERVATION CIRCUMSTANCES

UT DATE	OBJECT	PHASE ANGLE (deg)	SUB-EARTH (deg)		INTEGRATION TOTAL (min)
			Lon.	Lat.	
2000 July 18.35.....	Pluto	1.40	182	+24.6	169
2000 July 18.45.....	Triton	0.31	256	-50.0	64
2000 July 19.34.....	Pluto	1.42	126	+24.6	130
2000 July 20.34.....	Pluto	1.44	70	+24.6	194
2000 July 21.31.....	Pluto	1.46	15	+24.6	159
2000 July 21.39.....	Triton	0.22	76	-50.0	51
2000 July 22.26.....	Pluto	1.48	322	+24.6	78

were able to realize enormous gains in spectral resolution and signal precision compared with earlier efforts to observe Pluto and Triton at 3–4  $\mu\text{m}$ . We used the 2–4  $\mu\text{m}$  cross-dispersed mode of SpeX, which covers the *K* and *L* atmospheric transmission windows with six overlapping spectral orders. Midobservation circumstances appear in Table 1. Groups of target object observations were interspersed with groups of observations of solar analog stars BS 6060, 16 Cyg B, and Hyades 64.

Our software and procedures for spectral extraction have been described elsewhere (Grundy et al. 1999; Buie & Grundy 2000). Briefly, we used numerical profiles determined from observations of bright solar analog stars to perform optimal extraction (Horne 1986) from our spectral images of the stars, as well as from the much fainter observations of Pluto-Charon and Triton, all of which were obtained at the same two slit locations. Guiding on light reflected from the slit jaws enabled us to keep objects reliably centered in these two regions. We nodded back and forth between them at intervals ranging from 1 to 2 minutes. Spectra of solar analogs spanning a wide range of air masses were used to compute nightly wavelength-dependent extinction functions, which were used to correct all spectra from observed to zenith air mass. Groups of spectra for each target object were then robustly combined (robust estimation reduces sensitivity to outlier data, e.g., Buie & Bus 1992; Press et al. 1992), eliminating spurious data arising from defects in individual spectral images. These combined spectra were divided by similarly combined solar analog star spectra to produce spectra proportional to disk-integrated albedos. Scaling to geometric albedo was based on overlap between *K*-band portions of our spectra and recent, absolutely calibrated spectra from the literature (Cruikshank et al. 2000; Buie & Grundy 2000; Grundy & Buie 2002). Wavelength calibration was based on spectra of an internal arc lamp, as well as telluric absorption and emission lines and has a precision ranging from  $\pm 0.0004 \mu\text{m}$  at 2  $\mu\text{m}$  to  $\pm 0.0008 \mu\text{m}$  at 4  $\mu\text{m}$ , instrument flexure being the primary source of uncertainty. To overcome the extreme feebleness of the signal from Pluto and Triton in the *L* band, we binned our spectra using a  $\delta\lambda = 0.03 \mu\text{m}$  grid, so uncertainties in wavelength calibration are negligible in the resampled spectra.

### 3. ANALYSIS

Grand average *L*-band spectra are shown in Figure 1. The new data are broadly consistent with earlier observations (indicated by gray points from Spencer et al. 1990). The most prominent features evident in the new spectra of

both Pluto and Triton are strong  $\text{CH}_4$  absorptions near 3.3, 3.5, and 3.8  $\mu\text{m}$ , corresponding to methane's  $\nu_3$ ,  $\nu_2 + \nu_4$ , and  $2\nu_4$  vibrational transitions, as indicated in the figure.

Synthetic spectra were computed with a multiple scattering radiative transfer model (Hapke 1993), using parameters

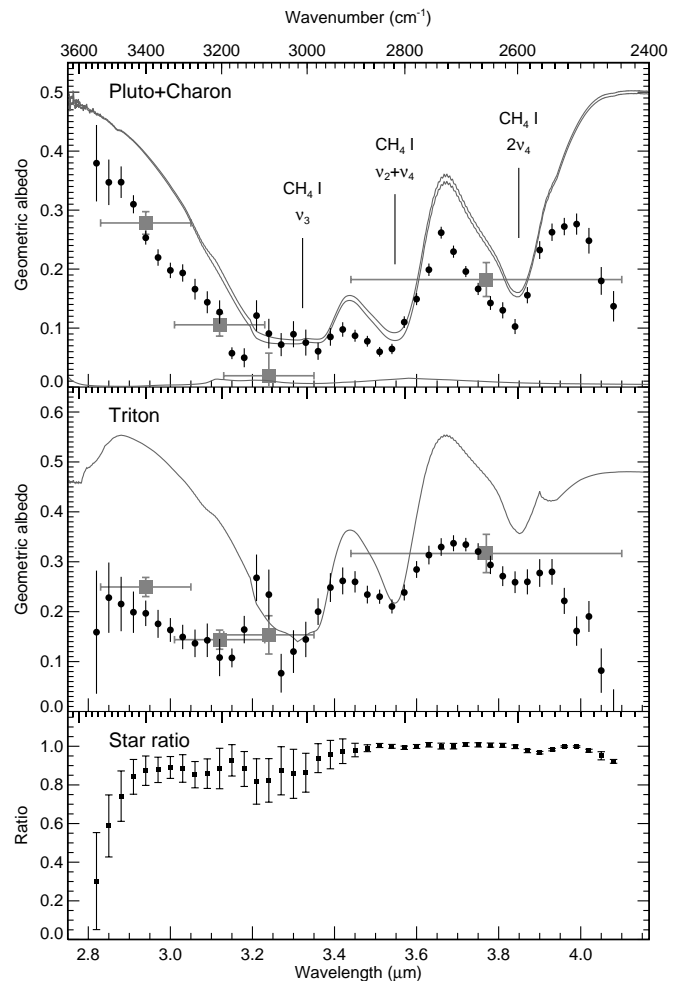


FIG. 1.—Grand average spectra of Pluto-Charon and Triton (*black circles*) compared with Spencer et al. (1990) data (*gray squares*), recent theoretical models (*gray curves*), and the wavelengths of three  $\text{CH}_4$  I bands. The models were computed from parameters presented by Douté et al. (1999) for Pluto, Buie & Grundy (2000) for Charon, and Quirico et al. (1999) for Triton. The separate contributions of Pluto and Charon models are shown, as well as their sum. Charon's contribution is minimal at these wavelengths. In the bottom panel, a ratio between solar analog stars observed at 1.84 and 1.15 air masses illustrates telluric transmission behavior.

from recent near-infrared models of the surfaces of Pluto (Douté et al. 1999, “ $R_{MCN}$ ” model), Charon (Buie & Grundy 2000), and Triton (Quirico et al. 1999, “best” model). Species used in these models include  $\text{CH}_4$  ice I (optical constants from Trotta 1996; Grundy, Schmitt, & Quirico 2002),  $\text{H}_2\text{O}$  ice  $I_h$  (optical constants from Trotta 1996),  $\text{CO}_2$  ice (optical constants from Hansen 1997),  $\beta$   $\text{N}_2$  ice (modeled as  $n = 1.22$ ,  $k = 0$ ), and  $\text{CO}$  ice (optical constants from Legay-Sommaire & Legay 1982; Quirico & Schmitt 1997b; Grundy & Buie 2001). These models are shown as gray curves in Figure 1. In gross form, the models match the observations, particularly with respect to the three broad  $\text{CH}_4$  ice absorption bands mentioned earlier. Just as at shorter infrared wavelengths, Pluto’s spectrum exhibits deeper  $\text{CH}_4$  bands than Triton’s does. Indeed, Pluto’s  $3.3 \mu\text{m}$   $\text{CH}_4$  band is so strongly saturated that it displays the broad, flattened bottom predicted by the Douté et al. (1999) model.

Our model spectra made use of optical constants for pure  $\text{CH}_4$  I, even for  $\text{CH}_4$  molecules isolated in  $\text{N}_2$  ice, a widespread phenomenon on Pluto and Triton (e.g., Quirico & Schmitt 1997a). Diluted in  $\text{N}_2$ , the absorption bands of  $\text{CH}_4$  shift toward shorter wavelengths. Unfortunately, optical constants for the  $\nu_3$ ,  $\nu_2 + \nu_4$ , and  $2\nu_4$  bands of methane diluted in the  $\beta$   $\text{N}_2$  ice phase are not available. One can get a rough idea of what size shift to expect from the following lines of evidence. In colder  $\alpha$  nitrogen ice, the shift on dilution of the  $\text{CH}_4$   $\nu_3$  band is about  $0.02 \mu\text{m}$  relative to the band’s location in pure  $\text{CH}_4$  I (Ewing 1964; Quirico & Schmitt 1997a). For  $\text{CH}_4$  bands observed in both  $\alpha$  and  $\beta$  nitrogen by Quirico and Schmitt (1997a), the shifts were generally smaller in the  $\beta$   $\text{N}_2$ . Extrapolating from observations of shifts in  $\beta$   $\text{N}_2$  of 19  $\text{CH}_4$  bands at wavelengths between 1 and  $2.5 \mu\text{m}$  (Quirico & Schmitt 1997a), one obtains expected shifts in the range of  $0.01 \mu\text{m}$  for the  $3\text{--}4 \mu\text{m}$   $\text{CH}_4$  bands. A shift of this magnitude would be smaller by a factor of 3 than our wavelength grid, so it should be barely discernible in our data, if present. Indeed, there does seem to be a slight shift, at least in the Pluto data. Higher spectral resolution observations are needed to confirm the presence of this shift and could potentially provide valuable constraints on the vertical structure of ices on Pluto and Triton. These absorption bands probe a very shallow surface layer compared with the weaker near-infrared  $\text{CH}_4$  bands. Comparison between the shifts of strong and weak  $\text{CH}_4$  bands could thus reveal if methane is most concentrated at the surface, as envisioned by Trafton, Matson, & Stansberry (1998) or if its concentration increases below the surface, as predicted by Grundy & Stansberry (2000).

Both models differ from the observed spectra in several wavelength regions, predicting less absorption than is observed between  $2.85$  and  $3.15 \mu\text{m}$  and also beyond  $\sim 3.6 \mu\text{m}$ . Additional absorbers are apparently present on the surfaces of Pluto and Triton, reducing albedos in these wavelength regions. We first consider what might be responsible for the shorter wavelength absorption and then turn to the longer wavelength absorption.

In the vicinity of  $2.9 \mu\text{m}$ , Triton’s albedo is significantly lower than Pluto’s, and both are lower than the model spectra. Both spectra show blue spectral slopes between  $2.8$  and  $3.1 \mu\text{m}$ .  $\text{H}_2\text{O}$  ice absorbs strongly in this region, as do complex organics, such as tholin-type radiolysis/photolysis residues (e.g., Khare et al. 1984, 1989; McDonald et al. 1993). The Quirico et al. (1999) Triton model shown in Figure 1

already contains considerable quantities of  $\text{H}_2\text{O}$  ice, covering 45% of the surface in an intimate mixture with  $\text{CO}_2$  ice. Likewise, Charon’s 22% of the total Pluto-Charon surface area is covered with  $\text{H}_2\text{O}$  ice. In spite of the presence of  $\text{H}_2\text{O}$  ice in these models, they predict insufficient absorption around  $2.9 \mu\text{m}$ , because  $\text{H}_2\text{O}$  in the models is restricted to only a fraction of each surface. To match the new data,  $\text{H}_2\text{O}$  must either be intimately mixed into much of the remaining surface regions of Pluto and Triton (regions also containing  $\text{N}_2$  and  $\text{CH}_4$  ices) or else those regions lacking  $\text{H}_2\text{O}$  ice must contain appreciable quantities of some other absorber, perhaps akin to tholin.

The presence of tholin has long been expected from the reddish visible-wavelength colors of Triton and Pluto (e.g., McEwen 1990; Thompson & Sagan 1990; Grundy & Fink 1996) and from the effects of photolysis and radiolysis on  $\text{CH}_4$  and  $\text{N}_2$  in the surfaces and/or atmospheres of Pluto and Triton (e.g., Delitsky & Thompson 1987; Stern, Trafton, & Gladstone 1988; Hudson & Moore 2001).

Figure 2 shows the effect of adding small quantities of Triton tholin (Khare et al. 1994) or  $\text{H}_2\text{O}$  ice to volatile-rich regions in the Douté et al. (1999) and Quirico et al. (1999) models ( $\text{H}_2\text{O}$  ice in previous models was restricted to regions lacking volatile ices). The models in this figure were produced by adding 0.02% tholin or 0.001%  $\text{H}_2\text{O}$  ice, dispersed at the molecular level within the  $\text{N}_2$  and  $\text{CH}_4$  ices of the Pluto and Triton models by means of linear combination of optical constants. As can be seen in Figure 2, even these minute quantities of tholin or  $\text{H}_2\text{O}$  dispersed in volatile-rich regions introduce substantial absorption around  $3 \mu\text{m}$ . However, the tholin provides a poor spectral match in

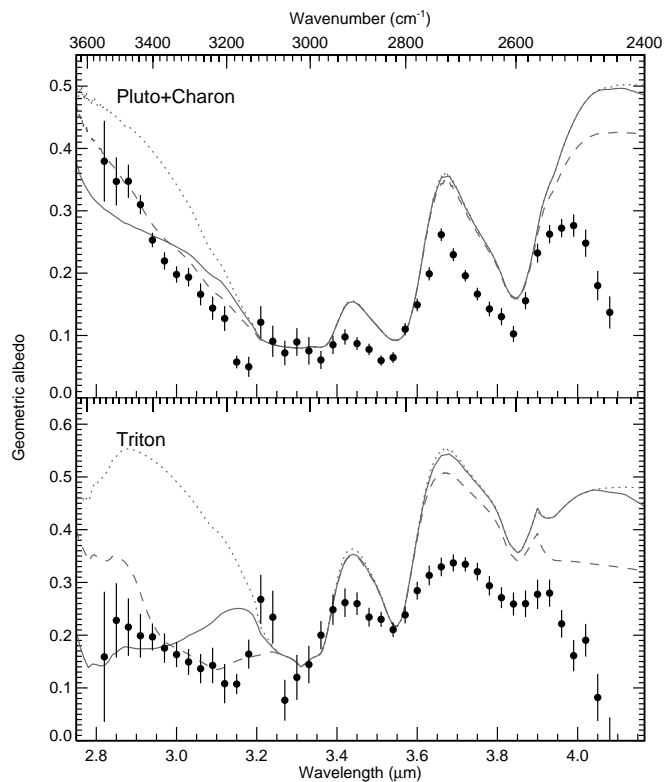


Fig. 2.—Observations compared with models having Triton tholin (solid curves) or  $\text{H}_2\text{O}$  ice (dashed curves) added to regions composed of volatile ices in the Douté et al. (1999) and Quirico et al. (1999) models from Fig. 2 (dotted curves).

this wavelength region, since it absorbs too strongly at wavelengths shorter than  $3 \mu\text{m}$ , relative to its absorption between  $3$  and  $3.2 \mu\text{m}$ . For this particular model configuration, we can place approximate limits of  $\leq 0.005\%$  tholin in  $\text{N}_2\text{-CH}_4\text{-CO}$  and  $\text{CH}_4$  terrains on both Pluto and Triton, if it is distributed uniformly (however, heterogeneous distributions could permit much higher tholin abundances). These tholin quantities are consistent with amounts required to produce the observed red slopes at visible wavelength and have little or no effect on near-infrared reflectances. Evidence of tholin abundance from  $3 \mu\text{m}$  and from visible wavelengths appear to be mutually consistent, but the addition of currently available tholin optical constants to existing models is not sufficient to explain the observed  $3 \mu\text{m}$  spectral profile of either body.

The addition of  $\text{H}_2\text{O}$  ice to volatile-rich regions of the Pluto and Triton models produces a much better match to the observed spectra than the tholins did. However, the mixture of  $\text{H}_2\text{O}$  ice and volatile ices is difficult to reconcile with the generally accepted picture of volatile  $\text{N}_2$ ,  $\text{CH}_4$ , and  $\text{CO}$  moving about on a substrate of refractory species like  $\text{H}_2\text{O}$  (e.g., Spencer et al. 1997). In the absence of other processes, volatile transport should efficiently segregate volatile from nonvolatile species.

At wavelengths longer than  $\sim 3.6 \mu\text{m}$ , the models also diverge from the spectral data, predicting albedos consistently higher than we observed. This discrepancy becomes quite severe beyond about  $3.95 \mu\text{m}$ , suggesting the presence of a previously unreported absorption band in this region. That Triton's albedo approaches zero near  $4.1 \mu\text{m}$  indicates that whatever absorber is responsible must have a nearly global distribution. Unfortunately, our spectra only extend to  $4.1 \mu\text{m}$  because of the grating setting we used for our observations, so we could not precisely determine the shape or central wavelength of the putative band. Relatively few species exhibit strong absorption near  $4 \mu\text{m}$  without also absorbing strongly at other near-infrared wavelengths. Two molecules that do have bands at  $4.1 \mu\text{m}$  are  $\text{CO}_2$  and  $\text{SO}_2$ , both of which are nonvolatile at Pluto and Triton surface temperatures, so as with  $\text{H}_2\text{O}$  ice, their global distribution would be unexpected in light of the prevailing picture of  $\text{N}_2$  and  $\text{CH}_4$  volatile transport. However,  $\text{CO}_2$  definitely does exist at least regionally on Triton's surface, having been detected from weaker, shorter wavelength absorption bands (Cruikshank et al. 1993).  $\text{CO}_2$  is included in the nonvolatile regions of the Quirico et al. (1999) model we employ here, but since  $\text{CO}_2$  only occurs on 45% of Triton's surface in the model, it does not produce sufficient absorption to explain the  $4 \mu\text{m}$  observations, as shown in Figure 1. Unlike  $\text{CO}_2$ ,  $\text{SO}_2$  has not been definitively detected on Triton or Pluto, but it has been suggested as a possible explanation for the shape of Pluto's UV spectrum (Stern 1993).

The spectral consequences of adding  $\text{CO}_2$  or  $\text{SO}_2$  to volatile-rich regions are explored in Figures 3 and 4. These figures show models produced by adding  $\text{CO}_2$  or  $\text{SO}_2$  to volatile-rich regions of the models having finely dispersed  $\text{H}_2\text{O}$  ice in Figure 2. Optical constants for  $\text{SO}_2$  ice were obtained from Schmitt et al. (1994) and from B. Schmitt (2001, private communication). For Triton, 0.02%  $\text{CO}_2$  or  $\text{SO}_2$  was added to the  $\text{N}_2\text{-CH}_4\text{-CO}$  region. For Pluto, 0.2%  $\text{CO}_2$  or  $\text{SO}_2$  was added to each model terrain containing  $\text{CH}_4$ , and we replaced the bright, neutral terrain with pure, fine-grained  $\text{CO}_2$  or  $\text{SO}_2$ . It should be noted that the Pluto  $\text{CO}_2$  model predicts observable  $\text{CO}_2$  absorption bands near

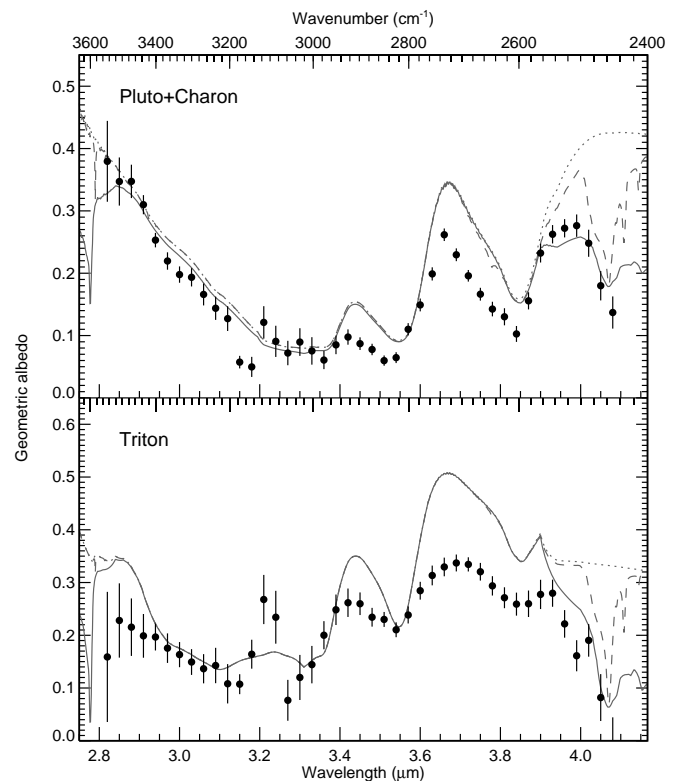


FIG. 3.—Observations compared with models having  $\text{CO}_2$  (solid curves) or  $\text{SO}_2$  (dashed curves) added to regions composed of volatile ices in the model with  $\text{H}_2\text{O}$  ice from Fig. 2 (dotted curves).

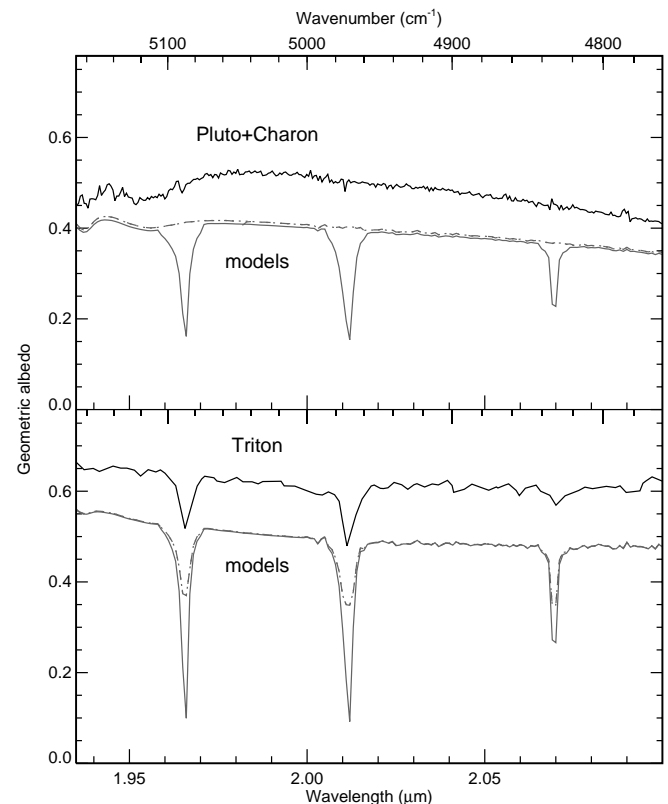


FIG. 4.—Same as Fig. 3, except at shorter wavelengths, and comparing with observations from other sources (black curves). Models (gray curves) are displaced down by 0.1. Note the absence of  $\text{CO}_2$  absorptions in a recent spectrum of Pluto-Charon (unpublished data recorded at IRTF/SpEx during 2001). The Triton spectrum is digitized from Cruikshank et al. (2000).

2  $\mu\text{m}$ . These bands are not seen (e.g., Fig. 4; Owen et al. 1993; Douté et al. 1999), so the Pluto/ $\text{CO}_2$  model seems to be ruled out, although perhaps a model based on a mixture of  $\text{CO}_2$  and  $\text{SO}_2$  could still be consistent with the near-infrared data. For Triton, the  $\text{CO}_2$  model also has difficulties, producing considerably deeper absorption in the 2  $\mu\text{m}$   $\text{CO}_2$  bands than is observed. While the inclusion of  $\text{CO}_2$  and/or  $\text{SO}_2$  improves the model fits to the 4  $\mu\text{m}$  observational data, neither species provides a perfect match in that region either. In particular, additional absorption is needed between 3.6 and 3.85  $\mu\text{m}$ .

Finally, around 3.2  $\mu\text{m}$ , both spectra show local maxima that are not matched by the model spectra. These features of the new data seem inconsistent with the Spencer et al. (1990) Pluto-Charon photometry, leading us to somewhat distrust our data in this wavelength region, which is also a site of strong telluric absorption by gaseous  $\text{CH}_4$  (see Fig. 1, bottom). Additional observations are needed to verify if these apparent features are spurious or real.

#### 4. DISCUSSION

The species we have added to volatile-rich regions of the models described above ( $\text{H}_2\text{O}$ ,  $\text{CO}_2$ , and  $\text{SO}_2$ ) are all nonvolatile at Triton and Pluto surface temperatures. Nonvolatile species are not expected to be involved in the volatile transport processes that rapidly redistribute  $\text{N}_2$ ,  $\text{CH}_4$ , and  $\text{CO}$  ices on Pluto and Triton, and thus they should tend to be left behind in regions experiencing volatile loss and tend to be buried under more mobile, volatile species in regions experiencing volatile deposition (e.g., Spencer et al. 1997). That our models seem to require nonvolatile species to be widely distributed in regions dominated by volatile species requires explanation. Two possibilities come to mind.

First, we could be seeing evidence for aeolian transport and subsequent incorporation of fine nonvolatile ice dust particles into the more volatile ices when they condense in the winter hemispheres of Pluto and Triton. Aeolian transport of small dust particles was considered by Sagan & Chyba (1990). They found that even an atmosphere as tenuous as Triton's 16  $\mu\text{bars}$  could move small, suspended dust particles long distances, and that particles smaller than 5  $\mu\text{m}$  could be lifted into suspension with expected surface wind velocities if cohesion between particles is small. Dust particles could also be injected into the atmosphere via eruptive processes, as observed on Triton (e.g., Soderblom et al. 1990). Optically, dust particles embedded in a volatile ice

matrix would inefficiently scatter radiation, because the contrast in refractive indices between the different ice species is small. Additionally, dust particles comparable to and smaller than the wavelength of incident light would be even less efficient scatterers. Small dust particles could thus impart their spectral absorption signature with little additional effect on radiative transfer within the icy surfaces of Pluto and Triton, consistent with our simple modeling approach.

Second, nonvolatile species such as  $\text{H}_2\text{O}$ ,  $\text{CO}_2$ , and tholins could be produced within volatile ice assemblages via photolysis and/or radiolysis of atmospheric or surface  $\text{CH}_4$ ,  $\text{CO}$ , and  $\text{N}_2$  (e.g., Strazzulla, Calcagno, & Foti 2001; Satorre, Palumbo, & Strazzulla 2001). If this mechanism were the explanation for the wide distribution of nonvolatile species, it would have important implications for rates of production versus burial under more volatile species. Production rates would have to be very high indeed to compete with burial by volatile transport cycles that operate on seasonal timescales.

#### 5. CONCLUSION

We present new IRTF/SpeX infrared reflection spectra of Pluto and Triton, covering the wavelength range 2.8–4.1  $\mu\text{m}$ . The new data exhibit strong  $\text{CH}_4$  absorption bands corresponding to the  $\nu_3$ ,  $\nu_2 + \nu_4$ , and  $2\nu_4$  vibrational transitions. The data reveal additional absorption not predicted by current models at wavelengths from 2.8 to 3.1  $\mu\text{m}$  and from 3.6 to 4.1  $\mu\text{m}$ . We tentatively attribute the additional 2.8–3.1  $\mu\text{m}$  absorption to  $\text{H}_2\text{O}$  ice and tholin in volatile-rich regions, while the additional 4  $\mu\text{m}$  absorption could be due to  $\text{CO}_2$  and/or  $\text{SO}_2$  ices in volatile-rich regions. These species are all refractory at Pluto and Triton surface temperatures, so one might expect them not to participate in seasonal cycles of volatile transport and thus be segregated from volatile ices, as assumed in earlier models. If they do indeed occur in volatile-rich regions on Pluto and Triton as the new data suggest, perhaps it is because they are being transported as fine dust particles by seasonal winds.

We thank W. Golisch and D. Griep for assistance at the telescope. This work was supported by NASA grants NAG 5-4210, NAG 5-9004, and NAG 5-10159 to Lowell Observatory, and by Hubble Fellowship HF-01091-97A from the Space Telescope Science Institute.

#### REFERENCES

- Bohn, R. B., Sandford, S. A., Allamandola, L. J., & Cruikshank, D. P. 1994, *Icarus*, 111, 151  
 Buie, M. W., & Bus, S. J. 1992, *Icarus*, 100, 288  
 Buie, M. W., & Fink, U. 1987, *Icarus*, 70, 483  
 Buie, M. W., & Grundy, W. M. 2000, *Icarus*, 148, 324  
 Cruikshank, D. P., Brown, R. H., Giver, L. P., & Tokunaga, A. T. 1989, *Science*, 245, 283  
 Cruikshank, D. P., Roush, T. L., Owen, T. C., Geballe, T. R., de Bergh, C., Schmitt, B., Brown, R. H., & Bartholomew, M. J. 1993, *Science*, 261, 742  
 Cruikshank, D. P., et al. 2000, *Icarus*, 147, 309  
 Delitsky, M. L., & Thompson, W. R. 1987, *Icarus*, 70, 354  
 Douté, S., & Schmitt, B. 1998, *J. Geophys. Res.*, 103, 31367  
 Douté, S., Schmitt, B., Quirico, E., Owen, T. C., Cruikshank, D. P., de Bergh, C., Geballe, T. R., & Roush, T. L. 1999, *Icarus*, 142, 421  
 Ewing, G. E. 1964, *J. Chem. Phys.*, 40, 179  
 Grundy, W. M., & Buie, M. W. 2001, *Icarus*, 153, 248  
 ———. 2002, *Icarus*, 157, 128  
 Grundy, W. M., Buie, M. W., Stansberry, J. A., Spencer, J. R., & Schmitt, B. 1999, *Icarus*, 142, 536  
 Grundy, W. M., & Fink, U. 1996, *Icarus*, 124, 329  
 Grundy, W. M., Schmitt, B., & Quirico, E. 2002, *Icarus*, 155, 486  
 Grundy, W. M., & Stansberry, J. A. 2000, *Icarus*, 148, 340  
 Hansen, G. B. 1997, *J. Geophys. Res.*, 102, 21569  
 Hapke, B. 1993, *Theory of Reflectance and Emittance Spectroscopy* (Cambridge: Cambridge Univ. Press)  
 Horne, K. 1986, *PASP*, 98, 609  
 Hudson, R. L., & Moore, M. H. 2001, *J. Geophys. Res.*, 106, 33275  
 Khare, B. N., Sagan, C., Arakawa, E. T., Suits, F., Callcott, T. A., & Williams, M. W. 1984, *Icarus*, 60, 127  
 Khare, B. N., Sagan, C., Heinrich, M., Thompson, W. R., Arakawa, E. T., Tuminello, P. S., & Clark, M. 1994, *BAAS*, 26, 1176  
 Khare, B. N., Thompson, W. R., Murray, B. G. J. P. T., Chyba, C. F., Sagan, C., & Arakawa, E. T. 1989, *Icarus*, 79, 350  
 Legay-Sommaire, N., & Legay, F. 1982, *Chem. Phys.*, 66, 315  
 McDonald, G. D., Thompson, W. R., Heinrich, M., Khare, B. N., & Sagan, C. 1994, *Icarus*, 108, 137  
 McEwen, A. S. 1990, *Geophys. Res. Lett.*, 17, 1765  
 Owen, T. C., et al. 1993, *Science*, 261, 745  
 Press, W. H., Teukolsky, S. A., Vetterling, W. T., & Flannery, B. P. 1992, *Numerical Recipes in C* (Cambridge: Cambridge Univ. Press)

- Quirico, E., Douté, S., Schmitt, B., de Bergh, C., Cruikshank, D. P., Owen, T. C., Geballe, T. R., & Roush, T. L. 1999, *Icarus*, 139, 159
- Quirico, E., & Schmitt, B. 1997a, *Icarus*, 127, 354
- . 1997b, *Icarus*, 128, 181
- Rayner, J. T., Toomey, D. W., Onaka, P. M., Denault, A. J., Stahlberger, W. E., Watanabe, D. Y., & Wang, S. 1998, *Proc. SPIE*, 3354, 468
- Sagan, C., & Chyba, C. 1990, *Nature*, 346, 546
- Satorre, M. A., Palumbo, M. E., & Strazzulla, G. 2001, *J. Geophys. Res.*, 106, 33363
- Schmitt, B., de Bergh, C., Lellouch, E., Maillard, J. P., Barbe, A., & Douté, S. 1994, *Icarus*, 111, 79
- Schmitt, B., Quirico, E., Trotta, F., & Grundy, W. M. 1998, *Solar System Ices*, ed. B. Schmitt, C. de Bergh, & M. Festou (Dordrecht: Kluwer), 199
- Soderblom, L. A., et al. 1990, *Science*, 250, 410
- Spencer, J. R., Buie, M. W., & Bjoraker, G. L. 1990, *Icarus*, 88, 491
- Spencer, J. R., Stansberry, J. A., Trafton, L. M., Young, E. F., Binzel, R. P., & Croft, S. K. 1997, *Pluto and Charon*, ed. S. A. Stern & D. J. Tholen (Tucson: Univ. Arizona Press), 435
- Stern, S. A. 1993, *Icarus*, 102, 170
- Stern, S. A., Trafton, L. M., & Gladstone, G. R. 1988, *Icarus*, 75, 485
- Strazzulla, G., Calcagno, L., & Foti, G. 1984, *A&A*, 140, 441
- Thompson, W. R., & Sagan, C. 1990, *Science*, 250, 415
- Trafton, L. M., Matson, D. L., & Stansberry, J. A. 1998, *Solar System Ices*, ed. B. Schmitt, C. de Bergh, & M. Festou (Dordrecht: Kluwer), 773
- Trotta, F. 1996, Ph.D. thesis, Univ. Joseph Fourier